NASA/CR-2002-212134
ICASE Report No. 2002-46

Self-consistent Physical Properties of Carbon Nanotubes in Composite Materials

R.B. Pipes
The University of Akron, Akron, Ohio

S.J.V. Frankland
ICASE, Hampton, Virginia

P. Hubert
McGill University, Quebec, Canada

E. Saether
NASA Langley Research Center, Hampton, Virginia

December 2002

The NASA STI Program Office . . . in Profile

Since its founding, NASA has been dedicated to the advancement of aeronautics and space science. The NASA Scientific and Technical Information (STI) Program Office plays a key part in helping NASA maintain this important role.

The NASA STI Program Office is operated by Langley Research Center, the lead center for NASA's scientific and technical information. The NASA STI Program Office provides access to the NASA STI Database, the largest collection of aeronautical and space science STI in the world. The Program Office is also NASA's institutional mechanism for disseminating the results of its research and development activities. These results are published by NASA in the NASA STI Report Series, which includes the following report types:

- TECHNICAL PUBLICATION. Reports of completed research or a major significant phase of research that present the results of NASA programs and include extensive data or theoretical analysis. Includes compilations of significant scientific and technical data and information deemed to be of continuing reference value. NASA's counterpart of peer-reviewed formal professional papers, but having less stringent limitations on manuscript length and extent of graphic presentations.

- TECHNICAL MEMORANDUM. Scientific and technical findings that are preliminary or of specialized interest, e.g., quick release reports, working papers, and bibliographies that contain minimal annotation. Does not contain extensive analysis.

- CONTRACTOR REPORT. Scientific and technical findings by NASA-sponsored contractors and grantees.

- CONFERENCE PUBLICATIONS. Collected papers from scientific and technical conferences, symposia, seminars, or other meetings sponsored or cosponsored by NASA.

- SPECIAL PUBLICATION. Scientific, technical, or historical information from NASA programs, projects, and missions, often concerned with subjects having substantial public interest.

- TECHNICAL TRANSLATION. English-language translations of foreign scientific and technical material pertinent to NASA's mission.

Specialized services that complement the STI Program Office's diverse offerings include creating custom thesauri, building customized data bases, organizing and publishing research results . . . even providing videos.

For more information about the NASA STI Program Office, see the following:

- Access the NASA STI Program Home Page at ***http://www.sti.nasa.gov***

- Email your question via the Internet to help@sti.nasa.gov

- Fax your question to the NASA STI Help Desk at (301) 621-0134

- Telephone the NASA STI Help Desk at (301) 621-0390

- Write to:
  NASA STI Help Desk
  NASA Center for AeroSpace Information
  7121 Standard Drive
  Hanover, MD 21076-1320

NASA/CR-2002-212134
ICASE Report No. 2002-46

Self-consistent Physical Properties of Carbon Nanotubes in Composite Materials

R.B. Pipes
The University of Akron, Akron, Ohio

S.J.V. Frankland
ICASE, Hampton, Virginia

P. Hubert
McGill University, Quebec, Canada

E. Saether
NASA Langley Research Center, Hampton, Virginia

ICASE
NASA Langley Research Center
Hampton, Virginia
Operated by Universities Space Research Association

Prepared for Langley Research Center
under Contract NAS1-97046

November 2002

Available from the following:

NASA Center for AeroSpace Information (CASI)
7121 Standard Drive
Hanover, MD 21076-1320
(301) 621-0390

National Technical Information Service (NTIS)
5285 Port Royal Road
Springfield, VA 22161-2171
(703) 487-4650

SELF-CONSISTENT PHYSICAL PROPERTIES OF CARBON NANOTUBES IN COMPOSITE MATERIALS

R. B. PIPES[1], S.J.V. FRANKLAND[2,3], P. HUBERT[4], AND E. SAETHER[5]

Abstract. A set of relationships is developed for selected physical properties of single-walled carbon nanotubes (SWCN) and their hexagonal arrays as a function of nanotube size in terms of the chiral vector integer pair, (n,m). Properties include density, principal Young's modulus, and specific Young's modulus. Relationships between weight fraction and volume fraction of SWCN and their arrays are developed for polymeric mixtures.

Key words. carbon nanotubes, density, modulus, hexagonal array, volume fraction, weight fraction, composites

Subject classification. Materials Science

Nomenclature

$\mathbf{a_1}$	unit vector
$\mathbf{a_2}$	unit vector
b	C-C bond length
E_n	Young's modulus of a SWCN (single-walled carbon nanotube)
E_{na}	Young's modulus of a hexagonal array of SWCN
$E_{\rho a}$	SWCN array specific modulus
$E_{\rho n}$	SWCN specific modulus
M_w	atomic weight of carbon
m	number of carbon atoms in a_2 direction
n	number of carbon atoms in a_1 direction
N	number of carbon atoms per unit length
N_a	Avogadro's number
R_n	SWCN radius
R_{na}	effective SWCN radius in and hexagonal array
R_{ne}	effective SWCN radius
V_a	SWCN volume fraction of the hexagonal array
V_n	SWCN volume fraction
W_a	SWCN array weight fraction
W_n	SWCN weight fraction
Y	graphene Young's modulus

[1] The University of Akron, Polymer Engineering Academic Center, Akron, OH 44325-0301.
[2] ICASE, NASA Langley Research Center, Hampton, VA 23681.
[3] This research was partially supported by the National Aeronautics and Space Administration under NASA Contract No. NAS1-97046 while S. J. V. Frankland was in residence at ICASE, NASA Langley Research Center, Hampton, VA 23681-2199.
[4] McGill University, Montreal, Quebec, H3A 2K6.
[5] NASA Langley Research Center, Hampton, VA 23681.

Λ chiral vector function
λ equilibrium separation distance between SWCN
ν equilibrium separation distance between SWCN and polymer
ρ_a SWCN array density
ρ_m SWCN/polymer composite density
ρ_n SWCN density
ρ_{na} SWCN density in a hexagonal array
ρ_p polymer density
$\overline{\rho}_a$ SWCN effective array specific gravity
$\overline{\rho}_n$ SWCN effective specific gravity

1. Introduction. The use of single-walled carbon nanotubes (SWCN) to further the reinforcement of polymeric materials is one of the current applications being explored [1,2] for this new material form since its discovery a decade ago [3]. In determining the nanotube contribution to the overall properties of a polymer composite, it is important to note that the 'effective fiber' is the nanotube or nanotube array, including their enclosed volume. This basic consideration affects a number physical properties of the composite such as the density, modulus, specific modulus, and the conversion between weight and volume fraction.

Considerable attention has been given to measuring and modeling the principal Young's modulus of carbon nanotubes. Some of these studies assume a nanotube shell, and others the enclosed nanotube volume. These different geometry definitions have led to reported values differing by almost two orders of magnitude [4-9]. For example, an experiment, determining the Young's modulus of the SWCN from vibrational analysis, assumed in the data analysis a nanotube shell of thickness 0.34 nm resulting in a Young's modulus of 1.25 TPa for SWCN of 1.0-1.5 nm in diameter [6]. AFM (atomic force microscopy) deflection experiments, which included the entire cross-section of the nanotube in the analysis, measured a Young's modulus of 1.31 TPa for an array 3 nm in diameter with the modulus dropping to 67 GPa for an array 20 nm in diameter [7]. The average diameter of individual SWCN in this study was 1.4 nm. The geometrical dependence of the nanotube modulus has been confirmed with theoretical calculations. Non-orthogonal tight-binding calculations based on a nanotube shell at a thickness of 0.34 nm, but parametrized for any shell thickness, yield 1.22-1.26 TPa for SWCN of 0.8-2.0 nm in diameter [8]. When the entire nanotube cross-section is included, molecular dynamics simulations of nanotubes in compression that utilize the Tersoff-Brenner potential for the C-C bonds, yield a Young's modulus of 1.5 TPa at SWCN diameter of ~0.5 nm which reduces to 0.2 TPa at a SWCN diameter of 4.0 nm [9].

The density of carbon nanotubes has been measured experimentally for randomly oriented nanotube arrays under high pressure [10]. Extrapolating to 1 atm, the density is close that expected of a perfect crystal lattice of SWCN reported as 1.33 g/cm^3. Another study reports a calculation of nanotube density based on assuming a shell geometry [11]. In the present work, a simple expression is derived for the density of an individual SWCN and a perfectly hexagonal crystalline array of SWCN in terms of both the radius and the chiral vector. With a given expression for density, it is further possible to develop a conversion between weight fraction and volume fraction of SWCN in a composite. This conversion is especially useful as a connection between theoretical predictions which tend to be in volume fraction, and experimental measurements which tend to be in weight (or mass) fraction.

One last consideration in the properties that will be reported here is the definition of nanotube size in the composite. Due to the chemical interactions of the polymer and the nanotubes, there is a small

equilibrium separation distance between the nanotube and either the surrounding polymer or other nanotubes in the SWCN array. This equilibrium separation distance is especially significant because the diameter of the nanotube is on the order of nanometers across. In this paper, the equilibrium separation distance between the nanotube and polymer is arbitrarily taken as 0.34 nm, the graphitic plane separation distance [12,13]. A value calculated in this work is used for the nanotube-nanotube equilibrium separation.

In this work, analytical expressions are derived for nanotube density, modulus, specific modulus and weight-volume fraction conversion assuming that the geometry of the nanotube or nanotube arrays includes all of the enclosed volume. This volume is dependent on the size of nanotube which is in turn dependent on the chirality (helicity) of the nanotube, generally described by the indices of its chiral vector (n,m) [14]. After a general description of nanotube geometry and nomenclature, each property will be addressed in turn for both SWCN and SWCN arrays: density, modulus, specific modulus, and weight-volume fraction conversion. These formulae provide a consistent set of relationships for use by researchers interested in calculating the effects of nanotube size on the effective properties of SWCN composites.

. **2. Geometry.**

2.1. SWCN. The SWCN has been described as a single graphene sheet rolled up with varying degrees of twist as described by its chiral vector, C_h:

$$\mathbf{C_h} = n\mathbf{a_1} + m\mathbf{a_2} \tag{2.1}$$

where a_1 and a_2 are the unit vectors of the two-dimensional hexagonal lattice and the indices "*n*" and "*m*" are integers [14]. These vectors and their summation are illustrated in Figure 2.1 for 3 specific examples of nanotubes. The solid lines perpendicular to the vector sum of a_1 and a_2 form the seam of the wrapped graphene sheet. The chiral vector C_h is also referred to by its indices as (n,m).

Nanotubes with chiral vectors of (n,n) and (n,0) have no twist and are classified as achiral nanotubes. These two special cases are sometimes denoted *armchair* and *zig-zag* respectively, referring to the pattern of the carbon atoms around the nanotube circumference [14]. Specific examples are included in Figure 2.1(a) for the vector diagram and structure (front and side views) of (6,6) armchair nanotube, and in Figure 2.1(b), for the (10,0) zig-zag nanotube where n=10. SWCN that do not fit either of these classifications are referred to as *chiral* nanotubes [14]. A (6,5) chiral nanotube is shown in Figure 2.1(c).

The SWCN radius, R_n, is a function of the integer pair, *n* and *m,* and the C-C bond length *b* [14]:

$$R_n = \frac{b}{2\pi}\sqrt{3}\Lambda \tag{2.2}$$

where

$$\Lambda = \sqrt{\left(n^2 + m^2 + mn\right)}. \tag{2.3}$$

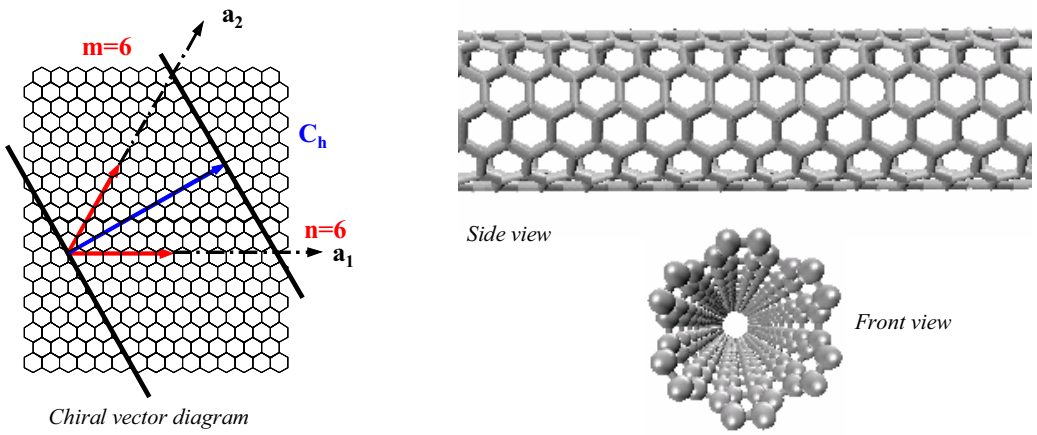

a) Armchair nanotube (6,6)

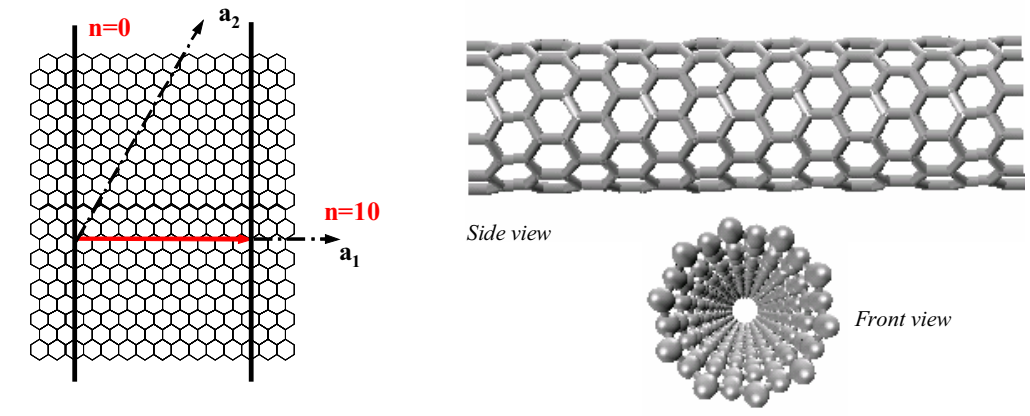

b) Zig zag nanotube (10.0)

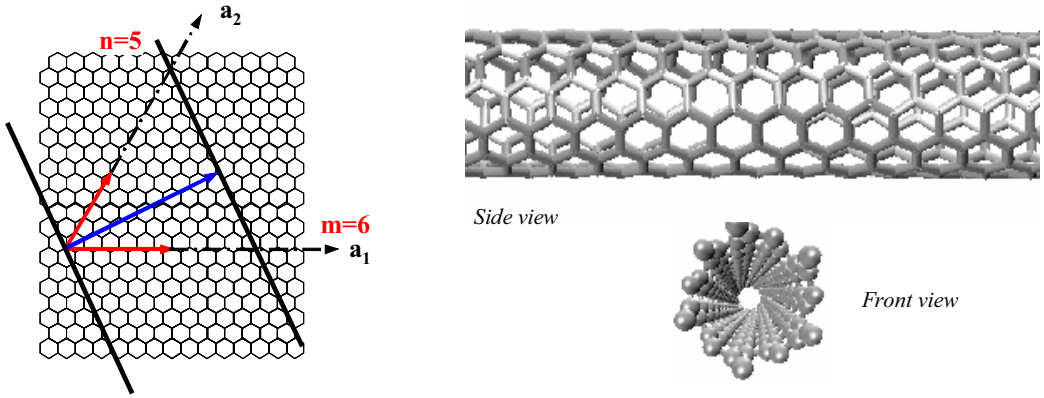

c) Chiral nanotube (6,5)

FIGURE 2.1. *SWCN structure and example of nanotubes.*

For the SWCN, the C-C bond length is equal to 0.142 nm [14]. This radius, R_n, does not the equilibrium separation distance, ν, between the nanotube and the surrounding polymer. Therefore, an effective radius, R_{ne}, is defined to include ν *as*

$$R_{ne} = \frac{b}{2\pi}\sqrt{3}\Lambda + \frac{\nu}{2} \quad . \tag{2.4}$$

The relation of R_n, R_{ne}, and ν, is shown in Figure 2.2(a) for the SWCN, and the resulting effective fiber cross-section in Figure 2.2(b). The surrounding polymer and the nanotube are each assigned one half of the equilibrium separation distance. The value of ν is dependent on the properties of the particular polymer, especially which functional groups of the polymer repeat unit are in the vicinity of the nanotube and how they align with respect to the nanotube. In the calculations a default value of 0.34 nm is used which is the separation of graphite planes [12, 13]. Other values from simulation force fields are considered.

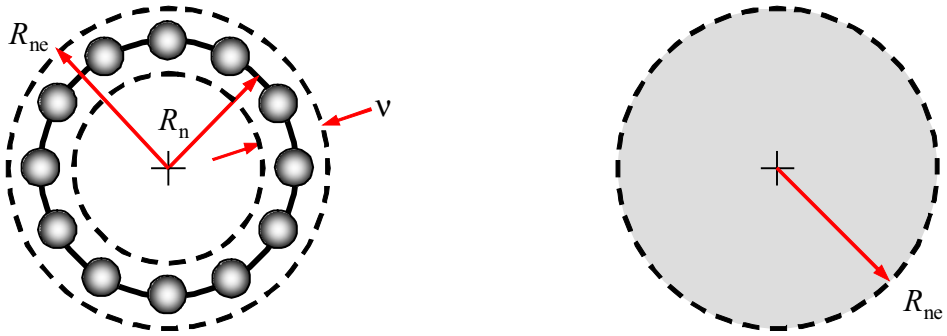

a) Open cylinder model of SWCN **b) Filled cylinder model of SWCN**

FIGURE 2.2. S*WCN nomenclature.*

2.2. SWCN Hexagonal Array. The synthesis of SWCN typically generates arrays of SWCN in a hexagonal cross-sectional arrangement [15]. For a SWCN in an array, the effective radius is

$$R_{na} = \frac{b}{2\pi}\sqrt{3}\Lambda + \frac{\lambda}{2} \tag{2.5}$$

where λ is the nanotube-nanotube equilibrium separation distance within the array analogous to ν specifically defined, in this work, for the polymer. The relation of R_n, R_{na}, and λ is shown in Figure 2.3(a) for the SWCN array, and the resulting effective fiber cross-section in Figure 2.3(b).

The value of λ was calculated for various SWCN arrays from molecular statics simulations using the method in Ref. 16. In these simulations, the potential energy of the array was minimized, using the Lennard-Jones potential (with parameters of ε=34.0 K and σ=0.3406 nm) to describe the nanotube-nanotube interactions. The results, summarized in Table 2.1, suggest that the separation distance is not strongly dependent on SWCN diameter, but rather can be taken as a constant equal to 0.318 nm in agreement with the equilibrium distance of 0.313 nm determined in Ref. [17] and 0.315 nm in Ref. [22]

TABLE 2.1

SWCN (n,0) Hexagonal Array Separation Distance.

n	Diameter (nm)	Separation Distance, λ (nm)
6	0.48	0.316
12	0.94	0.317
18	1.41	0.317
24	1.88	0.318
54	4.23	0.318
96	7.51	0.319

for a similar range of SWCN diameters. For a constant equilibrium separation distance, the SWCN volume fraction of the hexagonal array, $V_{a,}$ is a constant equal to the volume packing fraction of 0.906:

(2.6) $$V_a = \frac{\pi}{2\sqrt{3}} = 0.906$$

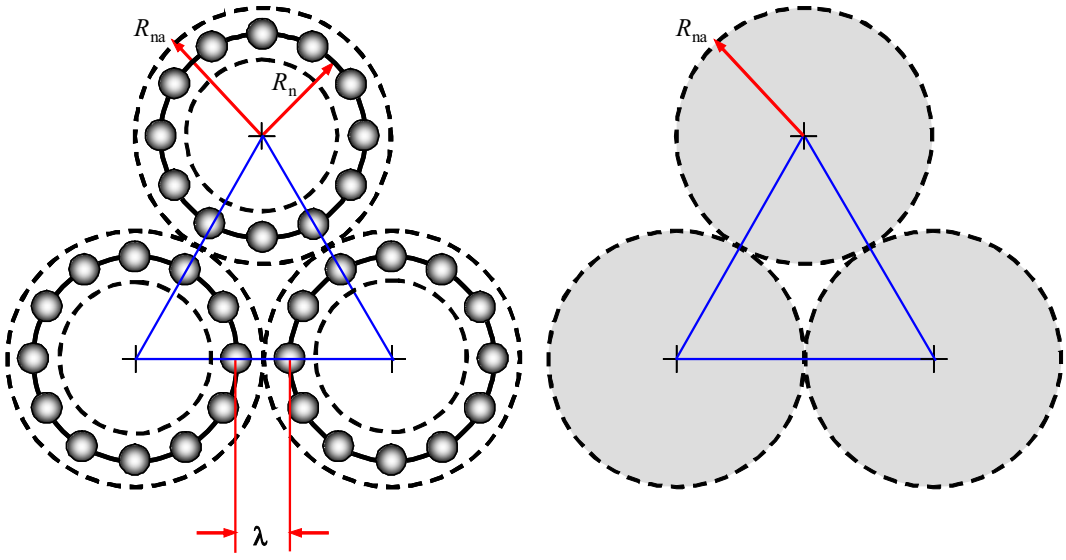

a) Carbon nanotube array b) Effective reinforcement array

FIGURE 2.3. *SWCN array nomenclature.*

3. Density. The density of SWCN is here derived from the mass of carbon atoms in the nanotube lattice per unit volume enclosed by the nanotube cylinder shown in Figure 2.2(b). The number of carbons per unit length is

(3.1) $$N = \frac{4\Lambda}{3b}$$

Combining equations (2.4) and (3.1), the nanotube density, $\rho_{n,}$ can be expressed in terms of the chiral vector as follows:

(3.2) $$\rho_n = \frac{NM_w}{\pi R_{ne}^2 N_a} = \frac{16\pi\Lambda M_w}{3b\left(3b^2\Lambda^2 + 2\sqrt{3}b\pi\Lambda\nu + \pi^2\nu^2\right)N_a}$$

where M_w is the molecular weight of carbon, N_a is Avogadro's number, and R_{ne} the effective radius which includes ν. For any particular polymer composite, the SWCN density is therefore dependent on the radius of the nanotube. This dependence of SWCN density on diameter is plotted in Figure 3.1 for ν=0.34 nm. Densities of specific nanotubes are marked with solid symbols. Over a range in diameter of 1-14 nm, that SWCN density decreases with increase in diameter by an order of magnitude. The SWCN density contribution is also dependent on the separation distance ν. In Table 3.1, a specific example of the sensitivity to ν is given for a (10,10) SWCN. For reference, the equilibrium separation distance for crystalline and amorphous polyethylene-nanotube composites with and without chemical bonds between the polymer and the nanotube is 0.38-0.42 nm. This range comes from molecular dynamics simulations of these composites and is determined from the separation of the nanotube peak from the first polymer peak in the radial distribution function. Details of the simulations can be found in Ref. [18]. The starting value of 0.25 nm was chosen because it is a typical hydrogen-hydrogen sigma parameter for the Lennard-Jones potential [19].

TABLE 3.1.
Density of a (10,10) SWCN in Different Matrices.

ν nm	**Density in g/cm^3**
0.25	1.602
0.30	1.506
0.32	1.471
0.33	1.453
0.34	1.436
0.35	1.419
0.36	1.403

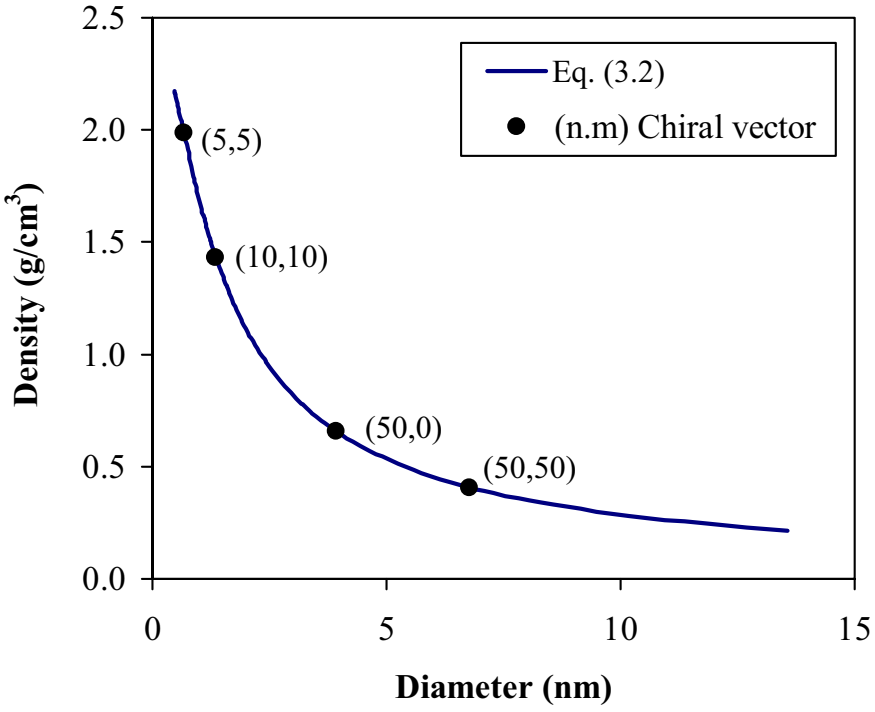

FIGURE 3.1. *SWCN density versus diameter.*

The density of a SWCN array is calculated by dividing the density of a single SWCN by the volume fraction of SWCN in the array which includes effective volume increase due to the nanotube-nanotube equilibrium separation distance λ. From equations (2.5), (2.6), and (3.1), SWCN array density is

$$\rho_a = V_a \rho_{na} = V_a \frac{N M_w}{\pi R_{na}^2 N_a} = \frac{\pi}{2\sqrt{3}} \left[\frac{16\pi\Lambda M_w}{3b\left(3b^2\Lambda^2 + 2\sqrt{3}b\pi\lambda\Lambda + \pi^2\lambda^2\right) N_a} \right] \tag{3.3}$$

Like the density of an individual SWCN, the array density shows a significant reduction with SWCN diameter. The density of a SWCN array differs from that of a SWCN only by a factor of the maximum volume fraction (0.906) and the difference in nanotube-polymer and nanotube-nanotube equilibrium separation distances.

4. Principal Young's Modulus. The principal Young's modulus is taken in the direction of the longitudinal axis of SWCN and its arrays. It is assumed in the following that the nanotubes are continuous and that the arrays consist of SWCN of identical diameter.

4.1. SWCN. A simple approach to calculating the Young's modulus of a SWCN is to map the stiffness of a graphene sheet onto the enclosing surface of the nanotube cylinder. The concept of using the graphene stiffness as a key parameter in calculating the Young's modulus of SWCN is not unique and has been used by others. (See for example, Refs. 7 and 20.)

To derive an expression which relates Young's modulus of the nanotube in terms of its chiral vector (n,m) as Λ directly to the graphene data, the modulus-area product of the effective modulus of the SWCN in the composite, E_n, as a filled cylinder of radius R_{ne} is set equal to that of a thin-walled cylinder of outer radius R_{ne}, thickness ν, and modulus Y of the graphene sheet. The effective modulus E_n can then be written as

$$E_n = \frac{8YR_n\nu}{4R_n^2 + 4R_n\nu + \nu^2} \tag{4.1}$$

$$where \quad Y = \frac{\left(C_{11}^2 - C_{12}^2\right)}{C_{11}}$$

where C_{11} and C_{12} are the stiffness constants of graphene [21]. Using equation (2.2) for R_n, equation (4.1) is rearranged as

$$E_n = \frac{4\sqrt{3}\pi bY\Lambda\nu}{3b^2\Lambda^2 + 2\sqrt{3}b\pi\Lambda\nu + \pi^2\nu^2} \tag{4.2}$$

Equation (4.2) can be derived from equation (1) in Ref. 20 if Y is used rather than C_{11}. In Figure 4.1, the Young's modulus of the SWCN from equation (4.2) is plotted as a function of diameter, taking Y=1029 GPa as the value of the Young's modulus of the graphene sheet and the separation distance as 0.342 nm [12]. Specific nanotube chiralities are marked with solid symbols in Figure 4.1. Equation (4.1) shows that the modulus of the SWCN decreases with increase in radius. A similar reduction in modulus with nanotube radius was derived from molecular dynamics simulation results of SWCN moduli using the Tersoff-Brenner potential to describe the C-C bonds [9]. In Table 4.1 a comparison of specific nanotube chiralities from equation (4.2) with the results of the graphene sheet model in Ref. 20 and the expression derived from molecular dynamics simulation results in Ref. 9 shows that the all three models provide very similar results.

TABLE 4.1

SWCN Young's Modulus for Specific Nanotube Chiralities.

Chiral	**Indices**	**SWCN**			**Arrays**	
n	**m**	**E_n Eq. (4.2) (GPa)**	**E_n Ref. 9 (GPa)**	**E_n Ref.20 (GPa)**	**E_a Eq.(4.3) (GPa)**	**E_a Ref. 7 (GPa)**
10	10	662	642	680	574	608
18	0	647	618	664	561	594
24	0	536	465	550	462	492
50	0	304	228	311	259	279
96	0	171	123	175	145	157

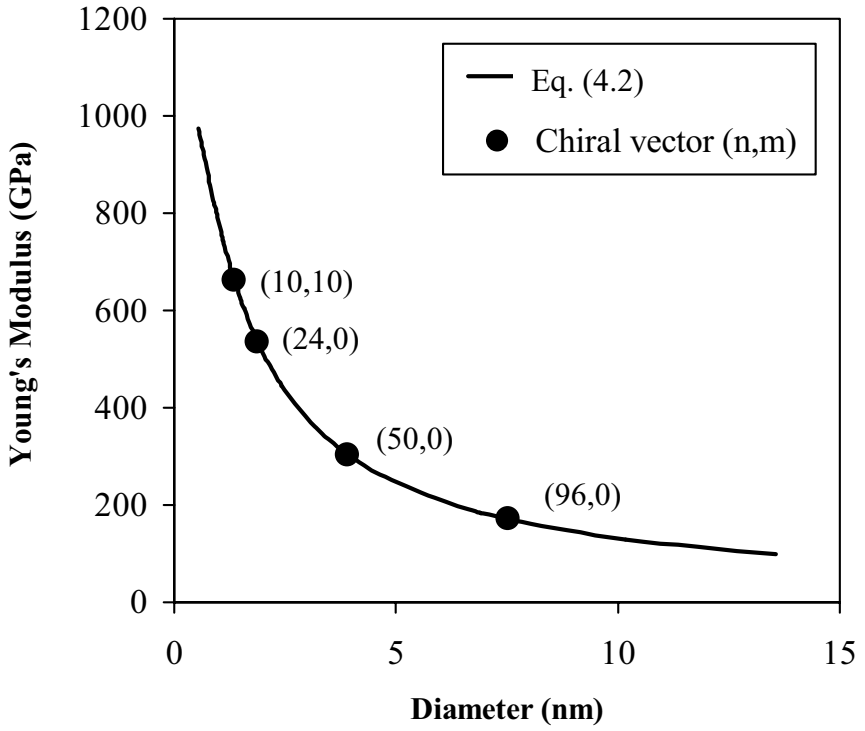

FIGURE 4.1. *Dependence of SWCN Young's Modulus on nanotube size.*

4.2 SWCN Hexagonal Array. The Young's modulus, $E_{a,}$ of a SWCN array containing SWCN with moduli described by equation (4.2) is obtained from equations (2.5), (2.6), and (4.2) as

$$E_a = V_a E_{na} = \frac{2\pi^2 bY\Lambda\lambda}{3b^2\Lambda^2 + 2\sqrt{3}b\pi\Lambda\lambda + \pi^2\lambda^2} \tag{4.3}$$

Values for the principal modulus of the SWCN array shown in Figure 4.2 are calculated from equation (4.3) and show that the array moduli follow identical trends to the individual SWCN. The array moduli differ from the SWCN moduli only by the product of the maximum volume fraction (0.906) and the difference in van der Waals distances (λ=0.318 nm vs. ν = 0.34 nm). In Table 4.1, a comparison is included of moduli calculated from equation (4.3) with those from the array graphene sheet model for SWCN arrays in Reference [7]. The model in Reference [7] differs from equation (4.3) by using C_{11} instead of Y and by using separate values for the graphene sheet thickness and the nanotube-nanotube separation distance. Furthermore, the values from equation (4.3) show excellent agreement with those calculated via a lattice dynamics method for selected armchair (3n,3n) and zig-zag (3n,0) SWCN [22]. Selected data points (solid symbols) from Ref. 22 are plotted with equation (4.3) in Figure 4.2.

5. Specific Axial Modulus. The specific modulus, $E_{\rho n,}$ of the SWCN is defined as the ratio of the principal Young's modulus, $E_{n,}$ to the dimensionless magnitude of the density, $\overline{\rho}_{\boldsymbol{n}}$, analogous to specific gravity. Combining equations (3.2) and (4.2) yields

(5.1) $$E_{\rho n} = \frac{E_n}{\overline{\rho}_n} = \frac{3\sqrt{3}b^2 Y \nu N_a}{4M_w}$$

Since the same geometry is utilized for calculating both modulus and density, the resulting equation (5.1) yields results independent of the SWCN diameter.

In a similar manner the specific modulus for the SWCN array, $E_{\rho a}$, is obtained by combining equations (3.3) and (4.4):

(5.2) $$E_{\rho a} = \frac{E_a}{\overline{\rho}_a} = \frac{3\sqrt{3}b^2 Y \lambda N_a}{4M_w} \ .$$

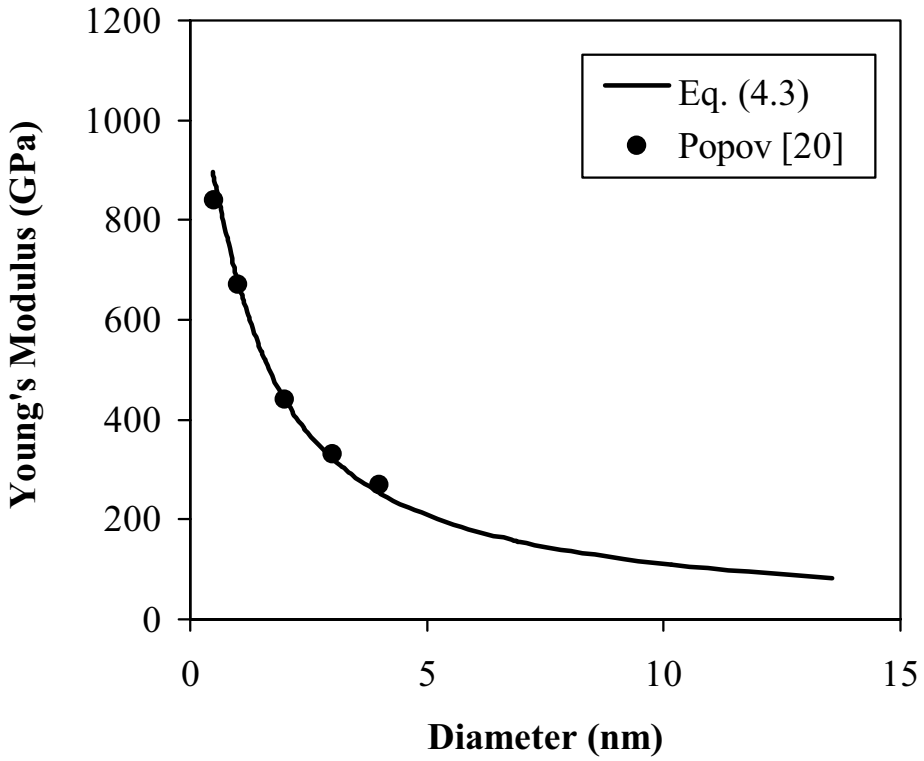

FIGURE 4.2. *Dependence of SWCN array axial modulus on nanotube size.*

These results show that the specific modulus of the SWCN array is, with the exception of the separation distance parameter, identical in form to that of the SWCN.

6. Weight Fraction/Volume Fraction Conversion. With an expression for the density of the SWCN, a relationship can be derived between weight fraction and volume fraction of SWCN in a composite. Consider a SWCN/polymer mixture of density, ρ_m with a SWCN volume fraction, V_n, a SWCN density of ρ_n and a polymer density of ρ_p. The SWCN volume fraction can be expressed as follows:

(6.1) $$V_n = \frac{\rho_m - \rho_p}{\rho_n - \rho_p}.$$

It is also possible to express the SWCN volume fraction in terms of its weight fraction, W_n, by definition:

(6.2) $$V_n = \frac{\rho_m}{\rho_n} W_n = \frac{W_n \rho_p}{W_n \rho_p + (1 - W_n)\rho_n}.$$

In terms of the chiral vector, equation (6.2) becomes

(6.3) $$V_n = \frac{W_n 3bN_a\left(3b^2\Lambda^2 + 2\sqrt{3}b\pi\Lambda\nu + \pi^2\nu^2\right)\rho_p}{W_n\rho_p 3bN_a\left(3b^2\Lambda^2 + 2\sqrt{3}b\pi\Lambda\nu + \pi^2\nu^2\right) + (1 - W_n)16\pi\Lambda M_w}.$$

This relationship between volume fraction and weight fraction for SWCN-polymer mixtures is plotted in Figure 6.1 (solid lines) for (6,6), (12,12) and (18,18) SWCN for a polymer density of 1 g/cm^3 in comparison to the V_n=W_n line (dotted). These curves show that as the diameter of the SWCN is increased the non-linearity in the relationship decreases. The influence of variations in polymer density upon the relationship between volume and weight fraction is shown in Figure 6.2 for the (10,10) SWCN in polymers of 0.8, 1.0, and 1.2 g/cm^3. Here increases in polymer density also reduce the non-linearity of the curves.

For SWCN arrays in a polymer mixture, a similar relationship between weight-fraction, W_a, and volume-fraction V_a can be derived as

(6.4) $$V_a = \frac{W_a 3\sqrt{3}bN_a\left(3b^2\Lambda^2 + 2\sqrt{3}b\pi\Lambda\nu + \pi^2\lambda^2\right)\rho_p}{W_n\rho_p 3\sqrt{3}bN_a\left(3b^2\Lambda^2 + 2\sqrt{3}b\pi\Lambda\nu + \pi^2\lambda^2\right) + (1 - W_n)8\pi^2\Lambda M_w}.$$

8. Conclusions. The overall set of analytical expressions presented here for the density, moduli, and weight-volume fraction conversion of nanotubes and nanotube arrays are derived as functions of the nanotube radius or chiral vector (n,m), and includes the equilbrium separation distance in the nanotube geometry to obtain the effective enclosed volume of the individual nanotube or array. The density and moduli of SWCN in polymer and SWCN arrays differ only by the array packing fraction and the equilibrium separation distances due to the chemical interactions between the nanotube and polymer or other nanotubes**.**

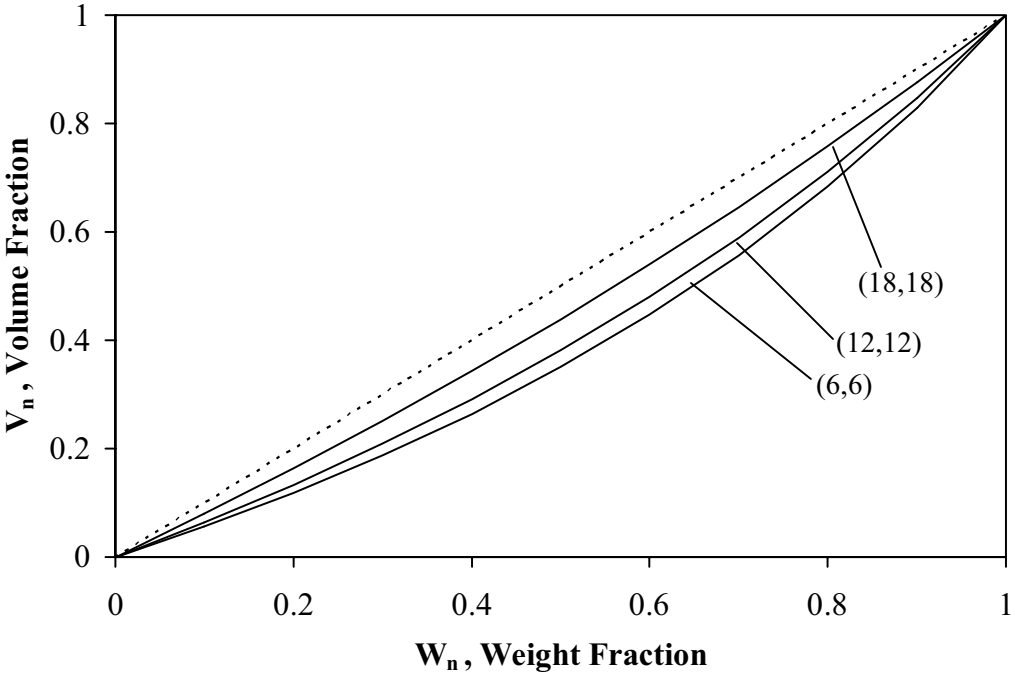

FIGURE 6.1. *SWCN volume fraction versus weight fraction (polymer density = 1 g/cm^3).*

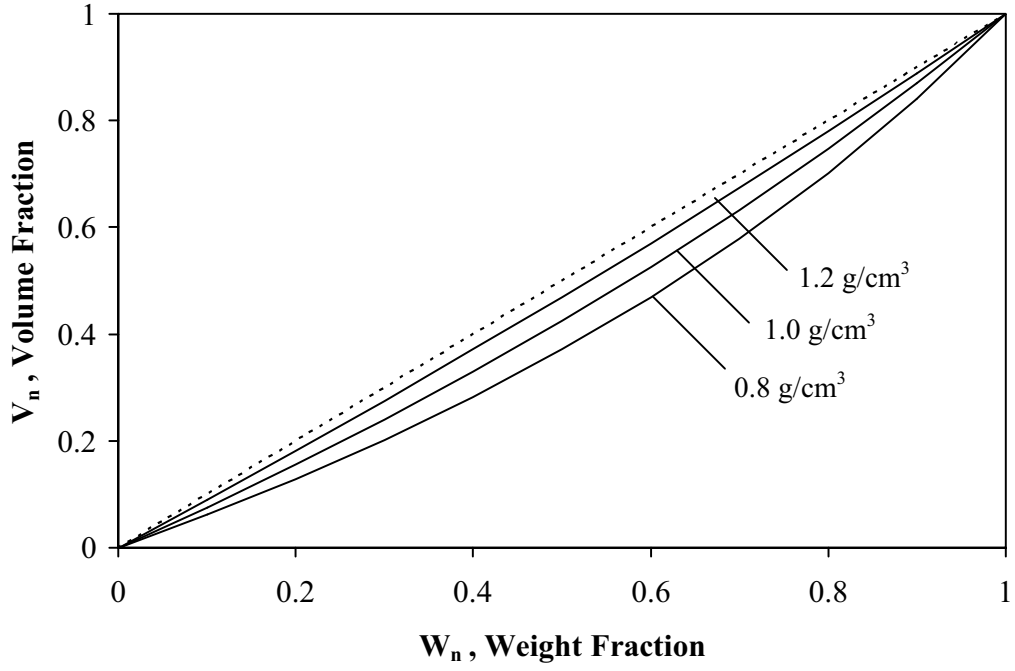

FIGURE 6.2. *SWCN (10,10) results for different polymer densities.*

A simple model for the SWCN principal modulus is derived assuming that the nanotube consists of a hollow cylinder with properties of the cylinder wall equal to the stiffness of the graphene sheet. This model agrees well with other graphene sheet models for SWCN and arrays in the literature, as well as published molecular dynamics simulation and lattice dynamics results. The modulus calculated from this model for both the SWCN and array shows an order of magnitude decrease over an increase in diameter from 1 to 14 nm. With this model, the specific modulus of both the SWCN and its hexagonal arrays was found to be independent of SWCN diameter.

Finally, a set of equations was derived for the relationship between weight fraction and volume fraction for SWCN and hexagonal arrays. The relationship requires knowledge only of the components of the chiral vector or radius of the SWCN and the weight fractions of the constituents to determine volume fraction of the SWCN or its hexagonal arrays in a mixture. For larger nanotubes in the same medium or the same size nanotubes in denser media the conversion curves becomes more linear and closer to a 1:1 conversion, assuming idealized, undeformed nanotubes**.**

Acknowledgment. R. B. Pipes and P. Hubert were supported by the National Aeronautics and Space Administration under NASA Cooperative Agreement NCC-1-02002.

REFERENCES

[1] E. T. THOSTENSON, Z. F. REN, and T. W. CHOU, *Advances in the science and technology of carbon nanotubes and their composites: A review*, Composite Science and Technology, 61 (2001), pp. 1899-1912.

[2] J. P. SALVETAT-DELMOTTE and A. RUBIO, *Mechanical Properties of carbon nanotubes: A fiber digest for beginners*, Carbon (2002), in press.

[3] S. IIJIMA, *Helical Microtubules of Graphitic Carbon*, Nature, 354 (1991), pp. 56.

[4] O. LOURIE and H. D. WAGNER, *Evaluation of Young's Modulus of carbon nanotubes by micro-Raman spectroscopy,* Journal of Materials Science, 13 (1998), pp. 2418-2422.

[5] D. SANCHEZ-PORTAL, E. ARTACHO, J. M. SOLER, A. RUBIO, and P. ORDEJON, *Ab initio structural, elastic, and vibrational properties of carbon nanotubes*, Phys. Rev. B, 59 (1999), pp. 12678-12688.

[6] A. KRISHNAN, E. DUJARDIN, T. W. EBBESEN, P. N. YIANILOS, and M. M. J. TREACY, *Young's modulus of single-walled nanotubes*, Phys. Rev. B, 58 (1998), pp. 14013-14019.

[7] J. P. SALVETAT, G. A. D. BRIGGS, J. M. BONARD, R. R. BACSA, A. J. KULIK, T. STOCKLI, N. A. BURNHAM, and L. FORRO, *Elastic and shear moduli of single-walled carbon nanotubes*, Phys. Rev. Lett, 82 (1999), pp. 944-947.

[8] E. HERNANDEZ, C. GOZE, P. BERNIER, and A. RUBIO, *Elastic properties of C and $B_xC_yN_z$ composite nanotubes*, Phys. Rev. Lett., 80 (1998), pp. 4502-4505.

[9] C. F. CORNWELL and L. T. WILLE, *Elastic properties of single-walled carbon nanotubes in compression,* Solid State Commun., 101 (1997), pp. 555-558.

[10] S. A. CHESNOKOV, V. A. NALIMOVA, A. G. RINZLER, R. E. SMALLEY, and J. E. FISCHER, *Mechanical energy storage in carbon nanotube springs*, Phys. Rev. Lett., 82 (1999), pp. 343-346.

[11] G. GAO, T. CAGIN, and W. A. GODDARD, *Energetics, structure, mechanical, and vibrational properties of single-walled carbon nanotubes*, Nanotechnology, 9 (1998), pp. 184-191.

[12] O. L. BLAKSLEE, D. G. PROCTOR, E. J. SELDIN, G. B. SPENCE, and T. WENG, *Elastic Constants of Compression-Annealed Pyrolytic Graphite,* J. Appl. Phys., 41 (1970), pp. 3373-3383.

[13] E. J. SELDIN and C. W. NEZBEDA, *Elastic Constants and Electron-Microscope Observations of Neutron-Irradiated Compression-Annealed Pyrolytic and Single-Crystal Graphite,* J. Appl. Phys., 41 (1970), pp. 3389-3400.

[14] M. S. DRESSELHAUS, G. DRESSELHAUS, and R. SAITO, *Physics of Carbon Nanotubes*, Carbon, 33 (1995), pp. 883-891.

[15] A. THESS, R. LEE, P. NIKOLAEV, H. DAI, P. PETIT, J. ROBERT, C. XU, Y. H. LEE, S. G. KIM, A. G. RINZLER, D. T. COLBERT, G. E. SCUSERIA, D. TOMANEK, J. E. FISCHER, and R. E. SMALLEY, *Crystalline ropes of metallic carbon nanotubes*, Science, 273 (1996), pp. 483-487.

[16] E. SAETHER, R. B. PIPES, and S. J. V. FRANKLAND, *Nanostructured composites: Effective mechanical property determination of nanotube bundles*, ICASE Report No. 2002-8, NASA/CR-2002-211461, April 2002.

[17] L. A. GIRIFALCO, M. HODAK, and R. S. LEE, *Carbon Nanotubes, Buckyballs, Ropes and a Universal Graphitic Potential*, Physical Review B, 62 (2000), pp. 13104-13110.

[18] S. J. V. FRANKLAND, A. CAGLAR, D. W. BRENNER, and M. GRIEBEL, *Molecular Simulation of the Influence of Chemical Cross-Links on the Shear Strength of Carbon Nanotube-Polymer Interfaces,* J. Phys. Chem. B, 106 (2002), pp. 3046-3048.

[19] M. P. ALLEN and D. J. TILDESLEY, *Computer Simulation of Liquids*, Clarendon Press, Oxford, 1987.

[20] R. S. RUOFF and D. C. LORENTS, *Mechanical and Thermal Properties of Carbon Nanotubes*, Carbon, 33 (1995), pp. 925-930.

[21] V. N. POPOV, V. E. VAN DOREN, and M. BALKANSKI, *Elastic properties of single-walled carbon nanotubes,* Phys. Rev. B, 61 (2000), pp. 3078-3084.

[22] V. N. POPOV, V. E. VAN DOREN, and M. BALKANSKI*, Elastic Properties of Crystals of Carbon Nanotubes,* Solid State Commun., 114 (2000), pp. 395-399.

REPORT DOCUMENTATION PAGE

Form Approved
OMB No. 0704-0188

1. AGENCY USE ONLY *(Leave blank)*	2. REPORT DATE	3. REPORT TYPE AND DATES COVERED
	December 2002	Contractor Report

4. TITLE AND SUBTITLE
SELF-CONSISTENT PHYSICAL PROPERTIES OF CARBON NANOTUBES IN COMPOSITE MATERIALS

5. FUNDING NUMBERS
C NAS1-97046
WU 505-90-52-01

6. AUTHOR(S)
R.B. Pipes, S.J.V. Frankland, P. Hubert, and E. Saether

7. PERFORMING ORGANIZATION NAME(S) AND ADDRESS(ES)
ICASE
Mail Stop 132C
NASA Langley Research Center
Hampton, VA 23681-2199

8. PERFORMING ORGANIZATION REPORT NUMBER
ICASE Report No. 2002-46

9. SPONSORING/MONITORING AGENCY NAME(S) AND ADDRESS(ES)
National Aeronautics and Space Administration
Langley Research Center
Hampton, VA 23681-2199

10. SPONSORING/MONITORING AGENCY REPORT NUMBER
NASA/CR-2002-212134
ICASE Report No. 2002-46

11. SUPPLEMENTARY NOTES
Langley Technical Monitor: Dennis M. Bushnell
Final Report
To be submitted to Composite Science and Technology.

12a. DISTRIBUTION/AVAILABILITY STATEMENT
Unclassified–Unlimited
Subject Category 34
Distribution: Nonstandard
Availability: NASA-CASI (301) 621-0390

12b. DISTRIBUTION CODE

13. ABSTRACT *(Maximum 200 words)*
A set of relationships is developed for selected physical properties of single-walled carbon nanotubes (SWCN) and their hexagonal arrays as a function of nanotube size in terms of the chiral vector integer pair, (n,m). Properties include density, principal Young's modulus, and specific Young's modulus. Relationships between weight fraction and volume fraction of SWCN and their arrays are developed for polymeric mixtures.

14. SUBJECT TERMS
carbon nanotubes, density, modulus, hexagonal array, volume fraction, weight fraction, composites

15. NUMBER OF PAGES
20

16. PRICE CODE
A03

17. SECURITY CLASSIFICATION OF REPORT	18. SECURITY CLASSIFICATION OF THIS PAGE	19. SECURITY CLASSIFICATION OF ABSTRACT	20. LIMITATION OF ABSTRACT
Unclassified	Unclassified		